Supramolecular Self-Assembly in a Disk-Cube Dyad Molecule Based on Triphenylene and Polyhedral Oligomeric Silsesquioxane (POSS)

Li Cui,[†] Jeffrey P. Collet,[†] Guoqiang Xu,[‡] and Lei Zhu*[,†]

Polymer Program, Institute of Materials Science and Department of Chemical, Materials, and Biomolecular Engineering, University of Connecticut, Storrs, Connecticut 06269-3136, and Baker Laboratory of Chemistry and Chemical Biology, Cornell University, Ithaca, New York 14853

Received February 17, 2006. Revised Manuscript Received May 18, 2006

An asymmetric disk-cube dyad molecule was synthesized by covalently attaching a 2-hydroxy-3,6,7,-10,11-pentakis(pentyloxy)triphenylene (P5T−OH) discotic molecule to a cubic polyhedral oligomeric silsesquioxane (POSS) molecule via a spacer. The sample was denoted as P5T−POSS. ^{1}H and ^{13}C nuclear magnetic resonance and size-exclusion chromatography were used to verify both its chemical structure and purity. On the basis of differential scanning calorimetry, two-dimensional (2D) X-ray diffraction (XRD), and transmission electron microscopy (TEM) analyses, we observed nanophase separation between the liquid crystalline P5T and crystalline POSS lamellae in the neat P5T−POSS and a miscible 1:1 mol/mol blend of P5T−POSS and POSS (denoted as 1:1 P5T−POSS:POSS). The melting temperatures of POSS crystals in P5T−POSS and 1:1 P5T−POSS:POSS were 62 and 66 °C, respectively. The isotropization temperature (T_i) of liquid crystalline P5T in P5T−POSS superposed with the POSS crystal melting at 66 °C, whereas it was at −5 °C in 1:1 P5T−POSS:POSS. The cubic POSS molecules in a planar hexagonal lattice stacked into an ABCA four-layer lamellar crystal, which had the same rhombohedral crystal structure (space group $R\bar{3}m$) as pure POSS crystals. Computer-simulated XRD for a lamellar model consisting of ABCA four-layer spheres and an amorphous lamella demonstrated that major crystal reflections, such as $(10\bar{1}1)$, $(11\bar{2}0)$, $(10\bar{1}2)$, and overlapped $(11\bar{2}3)/(30\bar{3}0)$, were still observable with the same *d*-spacing as those in pure POSS crystals. The discotic P5T molecules formed a bilayer liquid crystalline lamella between POSS lamellar crystals in P5T−POSS, whereas they interdigitated in the 1:1 P5T−POSS:POSS blend. Although no reflections related to columnar mesophases were observed in the 2D XRD patterns of P5T−POSS, the P5T discotic molecules were found to orient parallel to the lamellar normal in the confined space, reminiscent of a homeotropic nematic discotic structure.

Introduction

Self-assembly at different levels, ranging from atoms and molecules[1] to meso- and macroscopic materials,[2] has become an important strategy for the bottom-up nanotechnology in diverse applications. In the process of self-assembly, weak and noncovalent interactions are determining factors in finding the minimum free energy balanced between enthalpy and entropy terms, namely, chemical compatibility and structural (or shape) commensurability. Typical examples of supramolecular self-assembly are crystalline, liquid crystalline, and colloidal materials, where the large-amplitude motions of the molecules enables them to find a free-energy minimum in a thermodynamic pathway. Therefore, understanding fundamental self-assembly behaviors in condensed matters is crucial for the future development of nanotechnology.[3]

Molecular dyads with a dumbbell shape consist of two relatively big molecules covalently linked together via a chain or spacer. These two parts can be either symmetric or asymmetric. Asymmetric dyads are expected to show combined chemical and physical properties in particular. Because of their unique molecular shape and complementary property of the two parts, asymmetric dyads have attracted much attention for supramolecular self-assembly in molecular and nanodevices. Typical examples include dyad molecules of electron donor−acceptor pairs such as fullerene (C_{60})-containing dyads[4−7] and phthalocyanine−perylenediimide,[8] which have been intensively studied for their optoelectric properties in photovoltaic devices. Besides optoelectric properties, liquid crystalline dyads are also of interest for their self-assembly behaviors. Calamitic liquid crystalline dyads have been synthesized by attaching a fullerene to calamitic molecules.[9−11] In most cases, smectic A phases

* Corresponding author. E-mail: lei.zhu@uconn.edu. Tel: 860-486-8708.
[†] University of Connecticut.
[‡] Cornell University.

(1) Lehn, J.-M. *Supramolecular Chemistry*; VCH: Weihheim, Germany, 1995.
(2) Whitesides, G. M.; Boncheva, M. *Proc. Natl. Acad. Sci. U.S.A.* **2002**, *99*, 4769−4774.
(3) Tschierske, C. *Annu. Rev. Prog. Chem., Sect. C* **2001**, *97*, 191−267.
(4) Schuster, D. I. *Carbon* **2000**, *38*, 1607−1614.
(5) Gust, D.; Moore, T. A.; Moore, A. L. *J. Photochem. Photobiol., B* **2000**, *58*, 63−71.
(6) Imahori, H. *Org. Biomol. Chem.* **2004**, *2*, 1425−1433.
(7) Sanchez, L.; Herranz, M. A.; Martin, N. *J. Mater. Chem.* **2005**, *15*, 1409−1421.
(8) Fukuzumi, S.; Ohkubo, K.; Ortiz, J.; Gutierrez, A. M.; Fernandez-Lazaro, F.; Sastre-Santos, A. *Chem. Commun.* **2005**, 3814−3816.
(9) Chuard, T.; Deschenaux, R. *J. Mater. Chem.* **2002**, *12*, 1944−1951.

10.1021/cm060394e CCC: $33.50
Published on Web 06/23/2006

were observed with alternating C_{60} and liquid crystalline layers. Self-assembly behaviors of discotic liquid crystalline dyads in the bulk and on surfaces were investigated in hexa-*peri*-hexabenzocoronene (HBC)-containing systems.[12,13] In a HBC−pyrene dyad molecule, a hexagonal columnar (Col_h) phase was observed between 105 and 136 °C. The dyad molecule exhibited a more-ordered columnar phase at room temperature and a much lower isotropization temperature (T_i) than that of the pure HBC (T_i = 420 °C),[12] which enabled an easy processing in device fabrication. In HBC−anthraquinone dyads with various spacer lengths, oblique columnar (Col_o) phases existed at low temperatures and then transformed into Col_h phases at elevated temperatures.[13]

Polyhedral oligomeric silsesquioxane (POSS) molecules consist of silicon and oxygen atoms linked into a well-defined cubic cage with the silicon atoms at the corners and oxygen atoms interspersed along the edges. These materials have received increasing interest in the past decade, largely because of their well-defined structure of a 0.53 nm rigid inorganic core, which can be linked to eight functional groups to produce organic−inorganic hybrid structures.[14−16] Among these hybrid materials, novel organic−inorganic liquid crystals have been obtained by attaching mesogens to the inorganic POSS cores. Because of a restricted molecular topology imposed by the POSS cage, liquid crystalline POSS represents a promising candidate for the exploration of novel supramolecular self-assembly pathways in liquid crystals.[17]

Although the cubic framework of POSS led to a spherical organization of rodlike mesogens, lamellar or smectic morphology was often observed with alternating POSS and mesogen layers.[18−25] In combined mesogens and POSS systems, smectic phases were observed for end-attached mesogens, whereas lateral attachment of the mesogens resulted in a nematic phase.[18] When a POSS molecule was partially substituted with 4−5 calamitic mesogens, smectic A (SmA) phases were observed with occasional nematic phases for methoxyl-substituted biphenyl mesogens.[22,23] For an octa-substituted POSS with cyanobiphenyl mesogens, SmA phases were exclusively observed for various spacer lengths.[17,24] As the number of cyanobiphenyl mesogens increased to 16 per POSS molecule with a spacer length of $(CH_2)_{11}$, SmC and SmA phases were sequentially observed above the glass transition temperature (T_g).[25]

Because nematic liquid crystals are important for liquid crystal display industries, several methods have been attempted to obtain nematic mesophases for liquid crystalline POSS systems. The first method involved lateral attachment of calamitic mesogens to the POSS cores.[18] The second method used partial substitution of the cubic POSS cores.[22,23] The third method employed nematogenic mesogens in the systems.[26−28] When eight nonchiral nematogenic mesogens were linked to a POSS core, a nematic phase was observed above smectic-phase transitions.[26] When sixteen chiral nematogenic mesogens were laterally attached to the POSS core frames, a chiral nematic phase was observed at high temperatures (>100 °C), whereas rectangular and hexagonal columnar mesophases were found below 100 °C.[27] It was speculated that at low temperatures, the mesogens segregated at the peripheral of a cubic POSS core to form a giant disk with their directors roughly perpendicular to the disk plane. Further stacking of these donut-shaped disks led to columnar mesophase for these liquid crystalline POSS molecules. In the chiral nematic phase, the mesogens were supposed to couple with the POSS core to form an elongated (or ellipsoid) shape, whose director rotated successively along the helical axis. If the number of chiral mesogen groups reduced to eight, only chiral nematic mesophases were observed for two types of chiral sidearms in the nematogenic mesogens.[28]

However, there have not yet been investigations on liquid crystalline POSS containing discotic mesogens. Because discotic liquid crystals have exhibited unique electronic and optical properties and may be used as one-dimensional (1D) conductive wires when they form a column,[29] discogen−POSS dyads are a novel type of organic−inorganic hybrid material with potential in various applications. In this work, a triphenylene discotic molecule was covalently attached to a cubic POSS molecule through a C_{11} spacer to obtain an asymmetric dyad. The self-assembly behavior of this disk-cube dyad was characterized by X-ray diffraction (XRD) and transmission electron microscopy (TEM). Nanoscale microphase separation with alternating lamellar morphology was observed in the neat dyad molecule and its 1:1 mol/mol miscible blend with POSS, namely, the triphenylene disks formed a discotic nematic liquid crystalline layer after the POSS crystallized into a lamellar crystal. Most intriguingly, we reported for the first time that POSS molecules stacked into an ABCA four-layer lamellar crystal with the same rhombohedral crystal structure as that of pure POSS crystals. Computer-simulated XRD intensity proved that a single layer

(10) Campidelli, S.; Vazquez, E.; Milic, D.; Prato, M.; Barbera, J.; Guldi, D. M.; Marcaccio, M.; Paolucci, D.; Paolucci, F.; Deschenaux, R. *J. Mater. Chem.* **2004**, *14*, 1266−1272.
(11) Allard, E.; Oswald, F.; Donnio, B.; Guillon, D.; Delgado, J. L.; Langa, F.; Deschenaux, R. *Org. Lett.* **2005**, *7*, 383−386.
(12) Tchebotareva, N.; Yin, X.; Watson, M. D.; Samori, P.; Rabe, J. P.; Müllen, K. *J. Am. Chem. Soc.* **2003**, *125*, 9734−9739.
(13) Samori, P.; Yin, X.; Tchebotareva, N.; Wang, Z.; Pakula, T.; Jaeckel, F.; Watson, M. D.; Venturini, A.; Muellen, K.; Rabe, J. P. *J. Am. Chem. Soc.* **2004**, *126*, 3567−3575.
(14) Baney, R. H.; Itoh, M.; Sakakibara, A.; Suzuki, T. *Chem. Rev.* **1995**, *95*, 1409−1430.
(15) Phillips, S. H.; Haddad, T. S.; Tomczak, S. J. *Curr. Opin. Solid State Mater. Sci.* **2004**, *8*, 21−29.
(16) Laine, R. M. *J. Mater. Chem.* **2005**, *15*, 3725−3744.
(17) Goodby, J. W.; Mehl, G. H.; Saez, I. M.; Tuffin, R. P.; Mackenzie, G.; Auzely-Velty, R.; Benvegnu, T.; Plusquellec, D. *Chem. Commun.* **1998**, 2057−2070.
(18) Kreuzer, F.-H.; Maurer, R.; Spes, P. *Makromol. Chem., Macromol. Symp.* **1991**, *30*, 215−228.
(19) Mehl, G. H.; Goodby, J. W. *Angew. Chem., Int. Ed.* **1996**, *35*, 2641−2643.
(20) Saez, I. M.; Styring, P. *Adv. Mater.* **1996**, *8*, 1001−1005.
(21) Mehl, G. H.; Thornton, A. J.; Goodby, J. W. *Mol. Cryst. Liq. Cryst. Sci. Technol., Sect. A* **1999**, *332*, 2965−2971.
(22) Laine, R. M.; Zhang, C.; Sellinger, A.; Viculis, L. *Appl. Organomet. Chem.* **1998**, *12*, 715−723.
(23) Zhang, C.; Bunning, T. J.; Laine, R. M. *Chem. Mater.* **2001**, *13*, 3653−3662.
(24) Mehl, G. H.; Saez, I. M. *Appl. Organomet. Chem.* **1999**, *13*, 261−272.
(25) Saez, I. M.; Goodby, J. W. *Liq. Cryst.* **1999**, *26*, 1101−1105.
(26) Elsäber, R.; Mehl, G. H.; Goodby, J. W.; Photinos, D. J. *Chem. Commun.* **2000**, 851−852.
(27) Saez, I. M.; Goodby, J. W.; Richardson, R. M. *Chem.−Eur. J.* **2001**, *7*, 2758−2764.
(28) Saez, I. M.; Goodby, J. W. *J. Mater. Chem.* **2001**, *11*, 2845−2851.
(29) O'Neill, M.; Kelly, S. M. *Adv. Mater.* **2003**, *15*, 1135−1146.

of an ABCA stacking of the POSS molecules could show major XRD reflections with the same *d*-spacings as those of POSS crystals with a three-dimensional (3D) structure. In the liquid crystalline P5T layers, no columnar morphology was observed. The triphenylene disks formed a bilayer lamella in the pure dyad, whereas they interdigitated in its 1:1 (mol/mol) blend with POSS.

Experimental Section

Materials. 3-Hydroxypropylheptaisobutyl−POSS (iB−POSS−OH), 4-dimethyl-aminopyridine (DMAP), and 1,3-dicyclohexylcarbodiimide (DCC) were purchased from Aldrich and used without further purification. 1,2-Bis(pentyloxy)benzene was prepared according to the literature.[30] 2,3,6,7,10,11-Hexakis-(pentyloxy)triphenylene was prepared by trimerization of 1,2-bis(pentyloxy)-benzene using ferric chloride as an oxidative agent.[31] 2-Hydroxy-3,6,7,10,11-pentakis(pentyloxy)triphenylene (P5T-OH, **1**) was prepared by cleavage of 2,3,6,7,10,11-hexakis(pentyloxy)triphenylene with 1.2 equiv of B-bromocatecholborane.[32] Other commercially available chemicals were used without further purification.

Preparation of 11-(3,6,7,10,11-Pentakis(pentyloxy)triphenylene-2-oxy)undecanoic Acid (3). P5T−OH (0.4 g, 0.593 mmol) was added into a flask and dissolved with 6 mL of acetonitrile. Potassium iodide (20 mg, 0.120 mmol) and 0.45 g (3.26 mmol) of potassium carbonate were added. The temperature was then raised to 80 °C. Acetonitrile (2 mL) containing 0.183 g (0.655 mmol) of methyl 11-bromoundecanoate was added dropwise. The reaction was kept under reflux at 80 °C for 20 h. After being cooled to room temperature, the reaction mixture was filtered and washed with chloroform. The filtrate was collected, and the solvent was evaporated. Brown oil (**2**) was obtained and hydrolyzed with sodium hydroxide solution in ethanol at 70 °C for 3 h. The reaction mixture was neutralized with hydrochloric acid and then extracted with chloroform. After removing 11-bromoundecanoic acid by repeated precipitation in methanol, we obtained 0.45 g of product (**3**) with a yield of 88%. Proton nuclear magnetic resonance (^{1}H NMR) (δ, $CDCl_3$): 0.97 (m, 15H, CH_3), 1.34 (m, 10H, CH_3CH_2), 1.4−1.62 (m, 22H, $(CH_2)_6CH_2CH_2COO$ and $CH_3CH_2CH_2$), 1.71 (m, 2H, CH_2CH_2COO), 1.87 (m, 12H, OCH_2CH_2), 2.31 (t, 2H, CH_2COO), 4.25 (t, 12H, OCH_2), 7.82 (s, 6H, aromatic).

Preparation of P5T−POSS Dyad Molecule (5) and its 1:1 Blend with 11-Bromoundecanoyl iB−POSS (P5T−POSS:POSS). 3 (125 mg, 0.145 mmol), 97 mg of iB−POSS−OH (**4**, 0.112 mmol), and 15 mg of DMAP were added in a flask with 10 mL of CH_2Cl_2. DCC (145 mg, 0.703 mmol) was dissolved in about 2 mL of CH_2Cl_2 and added dropwise into the flask while the temperature was maintained at 0 °C. Slowly, the temperature was raised to reflux and stirred overnight. The reaction mixture was filtered, and the solvents were evaporated. The reaction mixture was purified by flash column chromatography with silica gel and an eluent of 1:5 acetone:hexane. The first fraction was collected, redissolved in acetone, and precipitated in methanol. A yellow solid was obtained and further purified with another silica gel column using toluene as eluent. The P5T−POSS dyad (80 mg) was obtained as a white waxlike solid. The yield was 42%. ^{1}H NMR (δ, $CDCl_3$): 0.61 (m, 16H, $SiCH_2$), 0.97 (m, 57H, CH_3), 1.24 (m, 2H, $COOCH_2CH_2$), 1.34 (m, 10H, CH_3CH_2), 1.4−1.62 (m, 22H, $(CH_2)_6CH_2CH_2COO$ and $CH_3CH_2CH_2$), 1.71 (m, 2H, CH_2CH_2COO), 1.86 (m, 12H, OCH_2CH_2), 1.97 (m, 7H, $SiCH_2CH$), 2.31 (t, 2H, CH_2COO), 4.04 (t, 2H, $COOCH_2$), 4.34 (t, 12H, OCH_2), 7.85 (s, 6H, aromatic). ^{13}C NMR (δ, $CDCl_3$): 14.1 (s, CH_3), 22.5 (s, $SiCH_2CH(CH_3)_2$, CH_3CH_2), 23.8 (s, $SiCH_2$), 25.0 (s, CH_2CH_2COO), 25.7 (s, $SiCH_2CH(CH_3)_2$), 28.4 (s, $CH_3CH_2CH_2$), 29.2 (m, OCH_2CH_2, $(CH_2)_7CH_2CH_2COO$), 29.5 (s, $SiCH_2$), 34.4 (s, CH_2COO), 66.2 (s, $COOCH_2$), 69.7 (s, OCH_2), 107.4 (s, 6C, aromatic), 123.6 (s, 6C, aromatic), 150.0 (s, 6C, aromatic), 173.8 (s, COO).

11-Bromoundecanoyl iB−POSS was synthesized via esterification of iB−POSS−OH with 11-bromoundecanoic acid using a method similar to that described above. It was obtained as a white solid with a yield of 67%. ^{1}H NMR (δ, $CDCl_3$): 0.61 (m, 16H, $SiCH_2$), 0.97 (d, 42H, CH_3), 1.30 (m, 12H, $(CH_2)_6CH_2CH_2Br$), 1.43 (m, 2H, CH_2CH_2COO), 1.56−1.72 (m, 4H, $COOCH_2CH_2$ and CH_2CH_2Br), 1.87 (m, 7H, $SiCH_2CH$), 2.30 (t, 2H, CH_2COO), 3.42 (t, 2H, CH_2Br), 4.04 (t, 2H, CH_2COO). It was blended with P5T−POSS in a 1:1 molar ratio in chloroform solution, and the solvent was fully evaporated in a vacuum oven at 50 °C before tests. The sample was denoted as 1:1 P5T−POSS:POSS.

Instrumentation and Characterization. ^{1}H and ^{13}C NMR spectra were recorded on a Bruker spectrometer (500 MHz, DMX 500), and $CDCl_3$ was used as solvent. Size-exclusion chromatography (SEC) was performed on a Viscotek GPCmax with a refractive index detector. THF was used as the solvent, and polystyrene standards were used for calibration. Differential scanning calorimetry (DSC) experiments were carried out on a TA DSC Q-100 instrument. An indium standard was used to calibrate the instrument. An approximately 3 mg sample was used for the DSC study, and the scanning rate was 5 °C/min. Wide-angle X-ray diffraction (WAXD) was performed using an X-ray tube generator operating at 1.6 kW with the Cr Kα radiation (wavelength λ = 0.229 nm). Two-dimensional (2D) data were recorded at room temperature, using a Bruker AXS area detector with a general area detector diffraction system (GADDS). The scattering vector q ($q = (4\pi\sin\theta)/\lambda$ where θ is the half-scattering angle) was calibrated with silver behenate with the first-order reflection at 1.076 nm^{-1}. Polarized light microscopy (PLM) experiments were performed using an Olympus BX51P microscope equipped with an Instec HCS410 hot stage. Simulation of the X-ray scattering intensity was carried out using MatLab 6.5. TEM experiments were performed on a Philips EM300 at an accelerating voltage of 80 kV. Thin sections with a thickness of ca. 70 nm were obtained using a Leica Ultracut UCT microtome equipped with a diamond knife at −30 °C. The thin sections were collected onto 400 mesh copper grids, freeze-dried, and stained by RuO_4 at room temperature for 30 min.[33]

Results and Discussion

Synthesis of P5T−POSS. The dyad P5T−POSS molecule was successfully synthesized as shown in Scheme 1. In the purification of **3**, repeated precipitation of the crude product in methanol should be performed to remove 11-bromoundecanoic acid, which was converted from the excess of methyl 11-bromoundecanoate used in the first step reaction. ^{1}H NMR was employed to monitor the disappearance of the impurity resonance from CH_2Br. This was essential for the synthesis of pure P5T−POSS product. Flash column chromatography was used twice to purify P5T−POSS. The excess of **3** was separated by first column chromatography with 1:5 acetone:hexane as eluent. A second column chro-

(30) Allen, M. T.; Diele, S.; Harris, K. D. M.; Hegmann, T.; Kariuki, B. M.; Lose, D.; Preece, J. A.; Tschierske, C. *J. Mater. Chem.* **2001**, *11*, 301−311.
(31) Boden, N.; Borner, R. C.; Bushby, R. J.; Cammidge, A. N.; Jesudason, M. V. *Liq. Cryst.* **1993**, *15*, 851−858.
(32) Kumar, S.; Manickam, M. *Synthesis* **1998**, 1119−1122.
(33) Trent, J. S.; Scheinbeim, J. I.; Couchman, P. R. *Macromolecules* **1983**, *16*, 589−598.

Scheme 1. Synthesis of an Asymmetric P5T−POSS Dyad Molecule

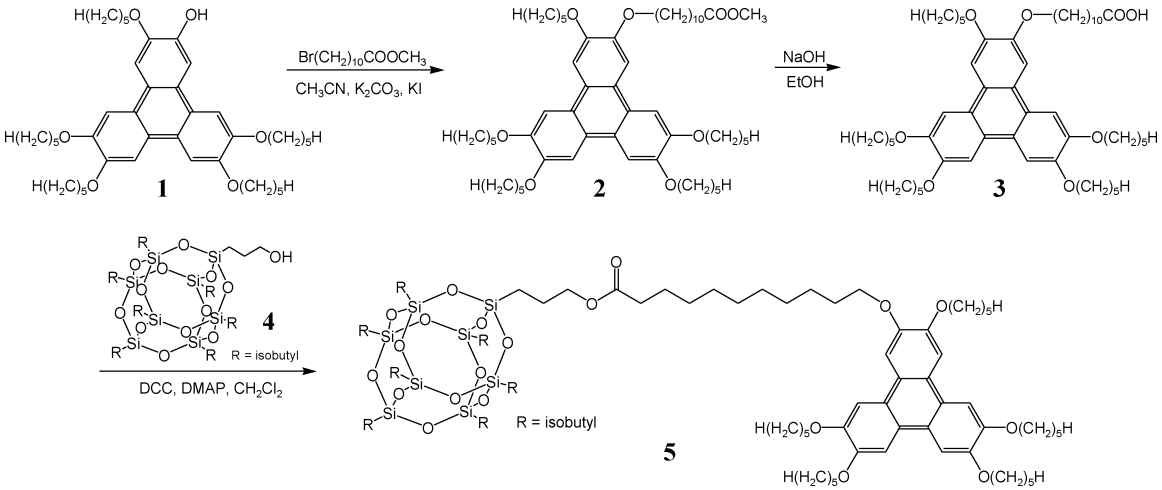

matography with toluene as the mobile phase was performed to separate the unreacted iB−POSS−OH from the P5T−POSS. SEC results of the P5T−POSS dyad, P5T−OH, and iB−POSS−OH are shown in Figure 1. As one can see, only

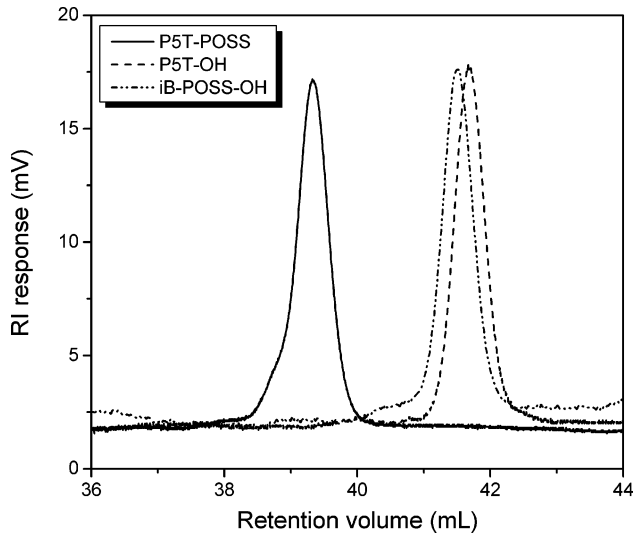

Figure 1. Size-exclusion chromatography curves for P5T−POSS, P5T−OH, and iB−POSS−OH, respectively.

a single peak was present for P5T−POSS, indicative of a high purity in the sample. Also, its retention volume was smaller than those for P5T−OH and iB−POSS−OH, suggesting a larger hydrodynamic volume and thus a higher molecular weight.

Thermal Behaviors of the Neat P5T−POSS and the 1:1 P5T−POSS:POSS Blend. DSC curves of P5T−POSS during the first cooling and second heating processes are shown in panels b and c of Figure 2. Upon cooling, a major crystallization peak was seen at 42 °C and a second transition was found at 36 °C. The overall heat of transition of both peaks was 13.2 kJ/mol. After peak deconvolution using Peakfit 4.0 software, the heat of transition for the major peak at 42 °C was 10.4 kJ/mol, whereas that for the minor peak at 36 °C was 2.8 kJ/mol. Because P5T is liquid crystalline and POSS is crystalline in their pure states, it is reasonable to attribute the lower temperature transition at 36 °C to the P5T liquid crystal formation and that at 42 °C to the POSS crystallization. Upon heating, the peak melting temperature (T_m) (and isotropization temperature, T_i) was 66 °C and the heat of fusion was 13.2 kJ/mol. Afterward, PLM showed no birefringence and no other transition was observed up to 300 °C (note that iB−POSS−OH has a major T_m at 275 °C, see the Supporting Information). It was obvious that the isotropization of P5T liquid crystals overlapped with the POSS crystal melting at 66 °C. The glass transition temperature (T_g) of the dyad was identified at −25 °C. It is interesting to note that the liquid crystal formation for the P5T has a supercooling of 30 °C, which is rare for typical isotropic-to-liquid-crystalline transitions. As discussed later, P5T forms a nematic phase only after microphase separation induced by POSS crystallization. Because POSS crystallization has a supercooling of 24 °C, the supercooling of 30 °C for the liquid crystalline P5T is thus understandable.

The P5T liquid crystalline transition and POSS crystal melting were much separated in the 1:1 P5T−POSS:POSS blend compared to P5T−POSS. The DSC curves of the 1:1 P5T−POSS:POSS during the first cooling and subsequent heating processes are shown in panels a and d of Figure 2. Upon cooling, a major POSS crystallization peak was seen at 46 °C (11.1 J/g), and a liquid crystalline transition for P5T was seen at −12 °C with an onset temperature at −6 °C (2.5 J/g). Upon subsequent heating, two melting peaks were seen at −5 °C (the onset temperature roughly at −8 °C) and 62 °C with heats of fusion being 2.5 J/g and 11.1 J/g, respectively. A careful inspection of the cooling and heating curves of 1:1 P5T−POSS:POSS indicated that the P5T liquid crystalline transition overlapped with a T_g around −20 °C. After normalization to the weight percentage of each component in the blend (P5T, 26.2 wt %; iB−POSS, 61.6 wt %; and spacer, 12.2 wt %), the P5T isotropization had a heat of fusion of 7.1 kJ/mol and the POSS crystal melting had a heat of fusion of 16.3 kJ/mol.

Comparing the thermal behaviors of P5T−POSS and 1:1 P5T−POSS:POSS, we found that the P5T liquid crystals in the neat P5T−POSS had a higher T_i but a smaller heat of fusion (2.8 kJ/mol) than that (7.1 kJ/mol) in the 1:1 P5T−POSS:POSS. Similarly, the POSS crystals in the P5T−POSS had a slightly higher melting temperature but a smaller molar heat of fusion (10.4 kJ/mol) than that (16.3 kJ/mol) in the

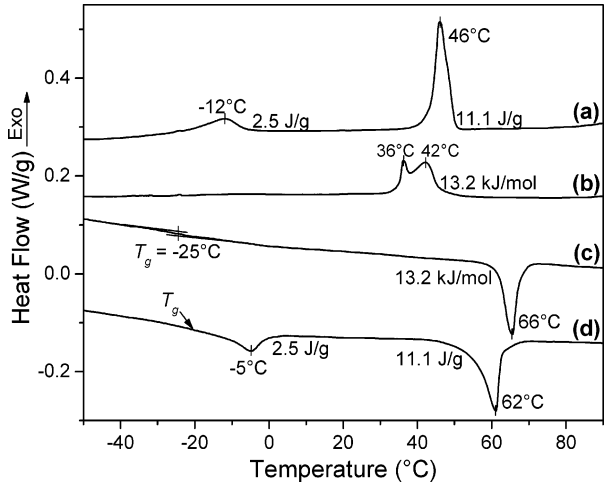

Figure 2. DSC thermograms for P5T−POSS during (b) the first cooling and (c) subsequent heating processes, and 1:1 P5T−POSS:POSS during (a) the first cooling and (d) subsequent heating processes. Both heating and cooling rates are 5 °C/min.

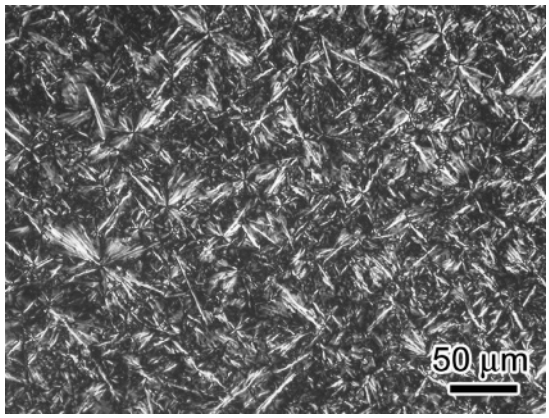

Figure 3. PLM micrograph of P5T−POSS at room temperature.

1:1 P5T−POSS:POSS blend. The lower T_i for the P5T liquid crystals in P5T−POSS:POSS suggested a lower thermodynamic stability for the P5T liquid crystals in the blend than in the neat dyad. However, higher heats of transition in the blend than in the neat dyad might be attributed to higher liquid crystallinity in the P5T and higher crystallinity in the POSS crystals.

The PLM observations of P5T−POSS at room temperature in Figure 3 showed poorly organized crystalline spherulites. Because the isotropization of P5T liquid crystals and melting of POSS superposed at 66 °C in neat P5T−POSS, this micrograph represented a state where P5T was liquid crystalline and POSS was crystalline. To reveal the liquid crystalline transition of P5T using PLM, we have given sample micrographs of 1:1 P5T−POSS:POSS at 0 and −30 °C in panels A and B of Figure 4, respectively. Note that both micrographs were recorded with identical exposure conditions. There was an abrupt increase in the brightness and contrast when the temperature decreased from 0 to −30 °C, indicating a liquid crystalline transformation for P5T, which further enhanced the birefringence in the sample. This result corresponded well with DSC results. The similar birefringence in Figures 3 and 4B for the dyad and the blend, respectively, further confirmed the existence of liquid crystalline P5T in the neat dyad at room temperature.

Phase Structures and Transitions Characterized by X-ray Diffraction and TEM. 2D XRD experiments on shear-oriented samples were used to determine the phase structures and morphology of P5T−POSS. The shear experiments were carried out at 45 °C, using two glass slides with samples sandwiched in between. A highly ordered lamellar structure was identified in the vertical direction from the X-ray patterns. Figure 5A demonstrates a 2D small-angle X-ray scattering (SAXS) pattern along the shear direction. Up to six orders of layer diffractions were observed on the meridian with an overall lamellar period of 6.0 nm. Note that the second-order diffraction was missing, possibly because of the form factor effect,[34] as the POSS and P5T layers might have similar thicknesses (see discussion below).

Pure POSS monomers decorated with eight alkyl attachments form a family of materials with structural similarities. The POSS molecules can be treated as spheres and they pack hexagonally into layers, which further stack into an ABC sequence instead of an AB sequence. Because it is not a close packing (i.e., face-centered cubic or fcc structure), the crystal system belongs to a trigonal (rhombohedral) structure with a space group of $R\bar{3}m$.[35−37] When the symmetry of the POSS monomer was broken by replacing one of the eight alkyl side groups with a functional group, asymmetric POSS molecules still fitted into the ABC-stacked rhombohedral crystal structure with slight variations in the unit-cell dimensions.[38,39] When POSS molecules were attached to polymers, XRD results showed that the POSS crystals in the hybrid polymers displayed the same major crystal reflections as those from pure POSS crystals.[40−43] Lamellar morphology with alternating bilayer POSS crystals and polymer lamellae was thus inferred.

First, 1D WAXD was employed to study the crystal structure and unit-cell dimensions of pure iB−POSS−OH and 11-bromoundecanoyl iB−POSS (see the Supporting Information). Two rhombohedral crystal structures with different unit-cell dimensions were observed for iB−POSS−OH. The major component crystal had unit cell dimensions of $a = 1.65$ nm, $c = 1.75$ nm, and $\alpha = 120°$. The minor component crystal unit-cell dimensions were tentatively determined as $a = 1.51$ nm, $c = 1.57$ nm, and $\alpha = 120°$, because only two major reflections (i.e., $(10\bar{1}1)$ and $(11\bar{2}0)$) were identified. Detailed crystal-structure determination will be carried out in the future, using the single-crystal XRD method. The rhombohedral unit-cell dimensions for 11-bromoundecanoyl iB−POSS were determined as $a = 1.63$

(34) Guinier, A.; Fournet, G. *Small Angle Scattering of X-rays*; Wiley: New York, 1955.
(35) Larsson, K. *Ark. Kemi.* **1960**, *16*, 203.
(36) Larsson, K. *Ark. Kemi.* **1960**, *16*, 209.
(37) Larsson, K. *Ark. Kemi.* **1960**, *16*, 215.
(38) Fu, B. X.; Hsiao, B. S.; Pagola, S.; Stephens, P.; White, H.; Rafailovich, M.; Sokolov, J.; Mather, P. T.; Jeon, H. G.; Phillips, S.; Lichtenhan, J.; Schwab, J. *Polymer* **2001**, *42*, 599−611.
(39) Waddon, A. J.; Coughlin, E. B. *Chem. Mater.* **2003**, *15*, 4555−4561.
(40) Zheng, L.; Waddon, A. J.; Farris, R. J.; Coughlin, E. B. *Macromolecules* **2002**, *35*, 2375−2379.
(41) Waddon, A. J.; Zheng, L.; Farris, R. J.; Coughlin, E. B. *Nano Lett.* **2002**, *2*, 1149−1155.
(42) Carroll, J. B.; Waddon, A. J.; Nakade, H.; Rotello, V. M. *Macromolecules* **2003**, *36*, 6289−6291.
(43) Zhang, L.; Hong, S.; Cardoen, G.; Burgaz, E.; Gido, S. P.; Coughlin, E. B. *Macromolecules* **2004**, *37*, 8606−8611.

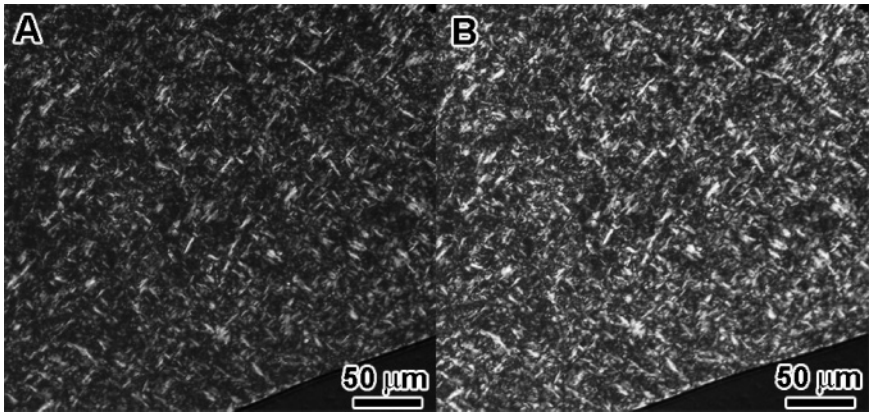

Figure 4. PLM micrographs of 1:1 P5T−POSS:POSS at (A) 0 °C and (B) −30 °C, respectively. Note that both micrographs were recorded with the same exposure conditions, and the difference in brightness and contract between two micrographs indicated the formation of liquid crystalline P5T as the temperature decreased from 0 to −30 °C.

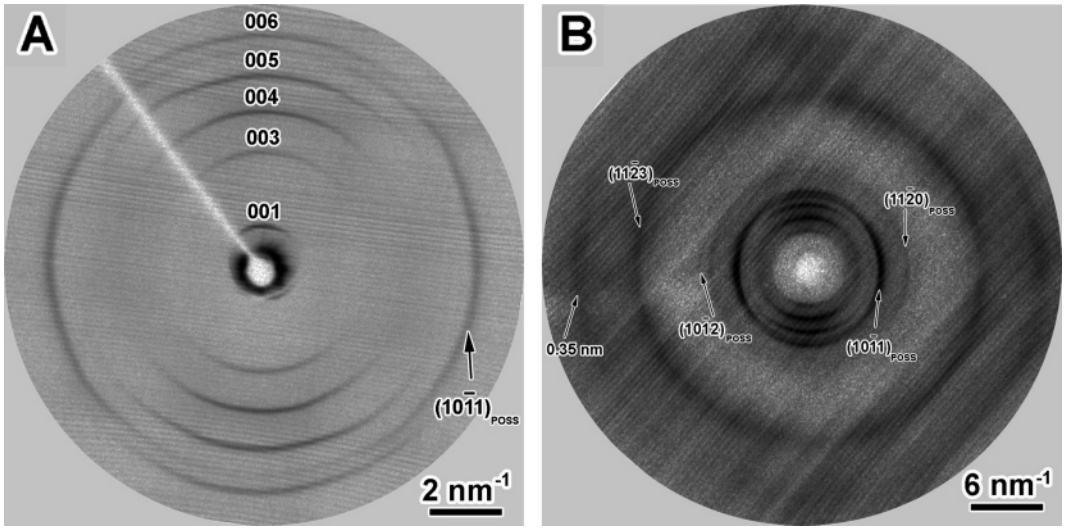

Figure 5. 2D (A) SAXS and (B) WAXD patterns along the shear direction for a shear-oriented P5T−POSS sample. The (11$\bar{2}$3) reflection is overlapped with the (30$\bar{3}$0) reflection in (B).

nm, $c = 1.71$ nm, and $\alpha = 120°$. From the WAXD pattern in Figures 5B, we could clearly identify reflections from POSS crystals, such as (10$\bar{1}$1), (11$\bar{2}$0), (10$\bar{1}$2), and overlapped (11$\bar{2}$3)/(30$\bar{3}$0), which had *d*-spacings similar to those of the 11-bromoundecanoyl iB−POSS crystals. The rhombohedral unit-cell dimensions for P5T−POSS were determined as $a = 1.63$ nm, $c = 1.73$ nm, and $\alpha = 120°$. In this rhombohedral unit cell, the POSS molecules (molecular diameter is ca. 1.0 nm) are not closely packed along the *a*-axis, as $c/a = 1.06$ is much smaller than the c/a value of 2.45 for a closely packed ABC stacking in the face-centered cubic structure. In the XRD patterns of the sheared sample in Figure 5B, the azimuthal scan results showed that the (10$\bar{1}$1) and (11$\bar{2}$0) reflections were centered on the equator, whereas the overlapped (11$\bar{2}$3)/(30$\bar{3}$0) was less oriented. A pair of reflections having a spacing of 0.35 nm was oriented on the equator in Figure 5B, which could be attributed to an average distance between parallel aligned neighboring triphenylene disks. Although the interdisk reflections were observed, no intercolumn reflections were seen in Figure 5A, indicative of an absence of a columnar mesophase for the triphenylene disks sandwiched between POSS crystals. Therefore, the P5T liquid crystalline phase can be assigned as a confined, homeotropic discotic nematic phase.

The crystalline structure of the lamellar POSS crystals sandwiched between discotic triphenylene layers is an important but still unsolved issue. Because each POSS molecule is attached covalently to a discotic molecule, the stacking number of hexagonally packed POSS layers should be no more than four. First, if the hexagonally packed POSS molecules stacked into a bilayer crystal with an AB (or AC) sequence, no (10$\bar{1}$1), (11$\bar{2}$0), (10$\bar{1}$2), or overlapped (11$\bar{2}$3)/(30$\bar{3}$0) reflections should be seen, because it belonged to a hexagonally close-packed structure instead of a rhombohedral structure. The observation of the (10$\bar{1}$1), (11$\bar{2}$0), (10$\bar{1}$2), and overlapped (11$\bar{2}$3)/(30$\bar{3}$0) reflections from POSS crystals suggested that each lamella of POSS crystals must have at least one unit-cell thickness, i.e., four layers of hexagonally packed POSS stacking into an ABCA sequence. The possibility of other stacking sequences such as ABAB (and ABAC) was unlikely, because they also belonged to a hexagonal structure with entirely different reflections.

From these XRD results, we can infer a lamellar morphology consisting of alternating POSS lamellar crystals and liquid crystalline P5T layers. Note that lamellar morphology with bilayer POSS crystals was also inferred in other reports for organic−inorganic nanocomposite polymers with POSS as pendant groups.[40−43] Taking into account the POSS (11$\bar{2}$0)

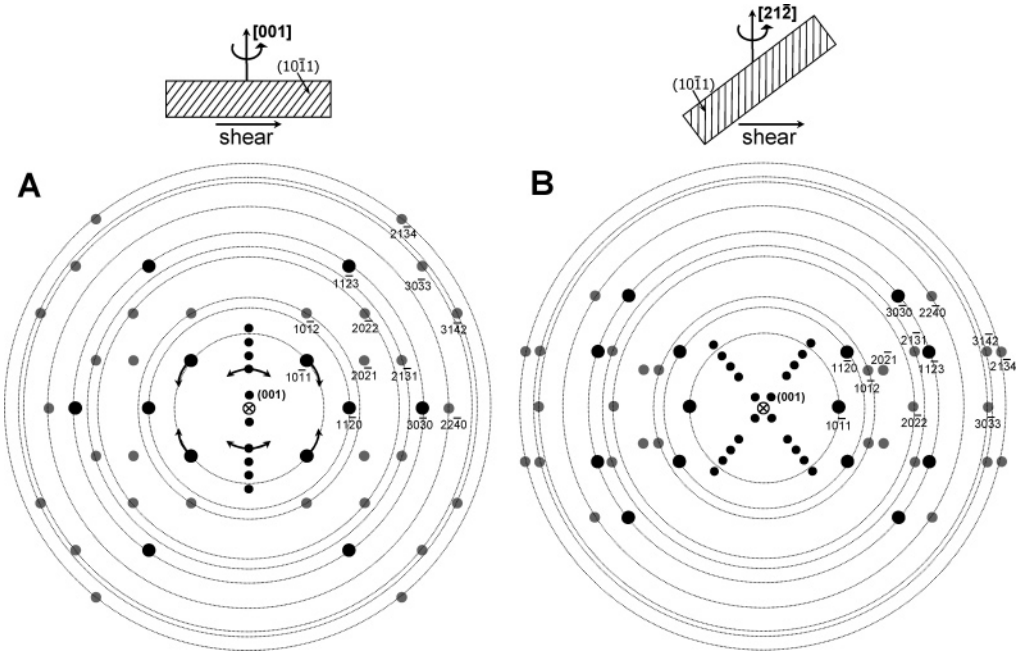

Figure 6. (A) Predicted [001] uniaxial X-ray pattern with layer reflections on the meridian. (B) Predicted [21$\bar{2}$] uniaxial X-ray pattern with the POSS (10$\bar{1}$1) reflections on the equator. The (10$\bar{1}$1) planes are represented by the tilted lines in the lamellar crystals on the top. Note that the layer reflections split into an "X" pattern, indicative of lamellar tilting. The spots in gray were not seen in Figure 5B for P5T−POSS but existed in Figure 8B for the 1:1 P5T−POSS:POSS blend.

reflection on the equator, we assume that the [001] direction should be parallel to the lamellar normal (or the meridian direction).[44] Figure 6A shows the predicted [001] uniaxial X-ray pattern with layer reflections in the vertical direction. From this predicted pattern, four POSS (10$\bar{1}$1) reflections should appear in the quadrant (i.e., 51° from the meridian). However, experimentally there was one maximum for the (10$\bar{1}$1) reflection on the equator with a broad distribution in the azimuthal scan profile. In the other extreme case, in Figure 6B, if the lamellae tilted an angle of 39° from the horizontal direction with the (10$\bar{1}$1) planes perpendicular to the shear direction, the POSS (10$\bar{1}$1) reflections would orient exclusively on the equator. The zone is determined as [21$\bar{2}$], which is found perpendicular to the (20$\bar{2}\bar{3}$) plane. In other words, (10$\bar{1}$1) reflections should move from the quadrant toward the equator, as the tilt angle gradually increased from 0 to 39° (see the arrows in Figure 6A). Note that twinning in rhombohedral crystals is a common phenomenon because of plastic deformation induced by various edge dislocations.[45] However, twinning along the (0003) plane is impossible for only four-layered ABCA POSS lamellar crystals, because twinning requires at least seven layers of ABCACBA stacking, with the middle A layer being the mirror plane. Therefore, no (10$\bar{1}$1) planes of the twin crystals should orient almost parallel to the horizontal direction (actually 12° tilted from the horizontal direction), and no (10$\bar{1}$1) reflections of the twin crystals are predicted in the vicinity of the meridian direction in Figure 6B. The basic feature of the predicted pattern in Figure 6B was the "X" layer reflections due to lamellar tilting. In the azimuthal scan profiles, however, the layer reflections had only a broad orientation distribution centering on the meridian. Therefore, neither of these two extreme cases in Figure 6 alone precisely accounted for our experimental observation in Figure 5B. However, if the POSS lamellar crystals had tilt angles between 0 and 39° with a broad orientation distribution (i.e., intermediate cases between the two extremes in Figure 6), the experimental pattern in Figure 5B would be satisfactorily explained.

On the basis of the above XRD results, a plausible lamellar model is illustrated in Figure 7a. In this model, POSS molecules self-assembled into an ABCA four-layer lamellar crystal sandwiched between triphenylene layers. Because the diameter of the POSS molecule was around 1.0 nm,[16] the four-layer POSS crystal thickness was estimated to be 2.7 nm (i.e., *c*-axis + diameter). The P5T layer thickness was thus 3.3 nm. Because one P5T disk had a diameter of ca. 1.7 nm, it suggested that there were two layers of parallel aligned P5T, as shown in Figure 7a. The P5T disks were tethered to the second layer POSS (dark gray) through the interstitials among three neighboring spheres in the top hexagonal layer. Because of the relatively short spacer length (C_{11} with an extended length of 1.4 nm), it was plausible to assume that the P5T disks tethered to the outer and inner POSS layers were staggered. This could account for the fact that no P5T columns were observed in the 2D XRD pattern in Figure 5.

The 2D SAXS and WAXD patterns for 1:1 P5T−POSS:POSS are shown in Figure 8. Again, lamellar morphology consisting of alternating P5T layers and ABCA-stacked POSS lamellar crystals was observed, because multiple layer

(44) In this study, we used four-parameter hexagonal indices (*hkil*) to describe a rhombohedral structure, where $i = -(h + k)$. However, instead of using the [*uvtw*] indices to represent the lattice directions, we adopt the [UVW] system, where $U = 2h + k = u - t$, $V = h + 2k = v - t$, and $W = 1.5l(a/c)^2 = w$. For details, refer to: Zhu, L.; Huang, P.; Chen, W. Y.; Cheng, S. Z. D.; Ge, Q.; Quirk, R. P.; Senador, T.; Shaw, M. T.; Thomas, E. L.; Lotz, B.; Hsiao, B. S.; Yeh, F.; Liu, L. *Macromolecules* **2003**, *36*, 3180−3188.

(45) Zhu, L.; Huang, P.; Cheng, S. Z. D.; Ge, Q.; Quirk, R. P.; Thomas, E. L.; Lotz, B.; Wittmann, J.-C.; Hsiao, B. S.; Yeh, F.; Liu, L. *Phys. Rev. Lett.* **2001**, *86*, 6030−6033.

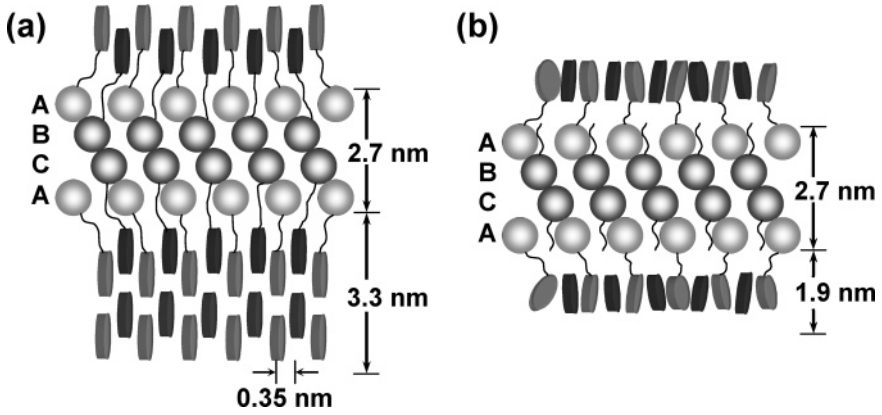

Figure 7. Schematic representations of (a) P5T−POSS and (b) 1:1 P5T−POSS:POSS self-assembly at room temperature, viewed along the $[100]_{POSS}$ direction. The POSS molecules stacked into a four-layer lamellar crystal with an ABCA stacking sequence. The liquid crystalline P5T disks formed a staggered bilayer in (a), whereas the isotropic P5T disks interdigitated in (b).

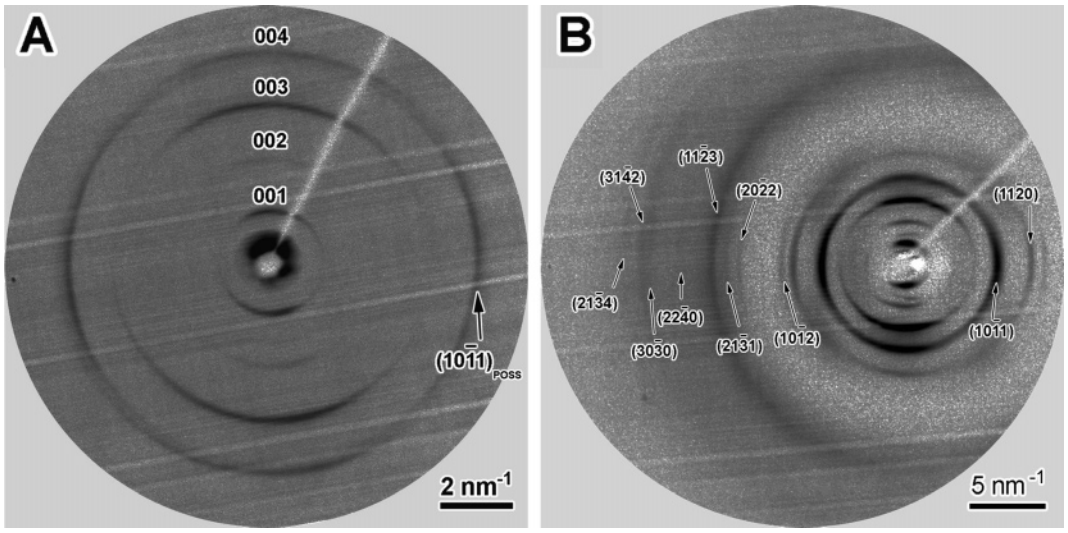

Figure 8. 2D (A) SAXS and (B) WAXD patterns along the shear direction for a shear-oriented 1:1 P5T−POSS:POSS blend. The (11$\bar{2}$3) reflection is overlapped with the (30$\bar{3}$0) reflection in (B).

reflections were seen on the meridian. The overall layer spacing was decreased to 4.6 nm, as compared to that (6.0 nm) for the neat P5T−POSS. However, 1:1 P5T−POSS:POSS showed higher crystallinity in the POSS crystals, as revealed by more POSS crystal reflections in Figure 8B than in Figure 5B. This is consistent with the DSC result that the heat of fusion for POSS crystals in 1:1 P5T−POSS:POSS was higher than that in P5T−POSS. On the basis of the 2D WAXD pattern in Figure 8B, the POSS lamellar crystals should also have an ABCA stacking sequence with a thickness of 2.7 nm, as shown in Figure 7b. Therefore, the P5T disk layer thickness was 1.9 nm, which could accommodate only one layer of P5T molecules, and thus an interdigitated morphology was obtained. In this liquid crystalline phase of P5T below <-5 °C, formation of a columnar phase was still unlikely, although there were no P5T molecules attached to the inner (B and C) POSS layers of the ABCA four-layer crystals. Because the spacer length (1.4 nm) is shorter than the neighboring POSS distance (1.63 nm), it is difficult for P5T molecules to pack into columns with a face-to-face interdisk spacing of 0.35 nm. We speculate that columnar phases could form only when the spacer length is long enough.

The molecular packing of discotic P5T in 1:1 P5T−POSS:POSS above the liquid crystal transition temperature at -5 °C (see the DSC result in Figure 2) is studied by a 1D WAXD in Figure 9, with a comparison to that of the neat P5T−POSS. In Figure 9, an interdisk spacing at 0.35 nm of parallel aligned triphenylene molecules is observed for the neat P5T−POSS, whereas only well-defined POSS crystalline peaks (30$\bar{3}$3) and (31$\bar{4}$2) are observed at a similar position for the 1:1 P5T−POSS:POSS blend. Therefore, it is reasonable to assign the P5T phase above -5 °C as an isotropic phase (see Figure 7b). In Figure 7b, we assume that the blended 11-bromoundecanoyl iB−POSS molecules formed the inner B and C layers, whereas the POSS molecules attached to P5T formed outer (or A) layers. These results also indicated that 1:1 P5T−POSS:POSS was a miscible blend and that the ABCA four-layer crystals resulted because of the equimolar ratio between P5T−POSS and iB−POSS.

The lamellar morphology in P5T−POSS is visualized in TEM micrographs in Figure 10A. Because P5T layers are liquid crystalline and POSS layers are crystalline, RuO_4 should stain the aromatic cores of P5T[33] more than the saturated hydrocarbon spacers[46] and the crystalline POSS

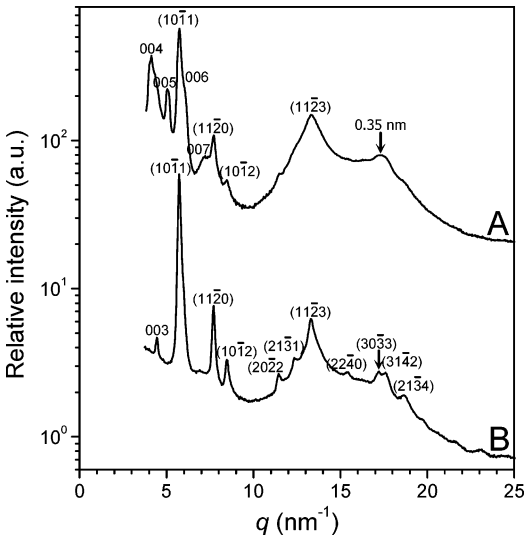

Figure 9. (A) 1D X-ray profile for P5T−POSS at 25 °C, where the P5T is liquid crystalline. (B) 1D X-ray profile for 1:1 P5T−POSS:POSS at 25 °C, where the P5T is isotropic.

layers. In the inset of Figure 10A, indeed, the bright layers (crystalline POSS and spacers) are slightly thicker than the dark layers (aromatic cores of P5T). From the TEM micrograph, it can be seen that the lateral grain sizes of the lamellae were relatively small (50−150 nm) and their orientation along the shear direction was not uniform. It was because of the small grain sizes of the microdomains that uniform orientation was difficult to achieve during mechanical shear, and this would explain the less-perfect orientation in the X-ray patterns in Figure 5B. It is surprising that although the lateral grain sizes are relatively small, up to six orders of lamellar reflections are still observed in the XRD experiments. A similar phenomenon was also observed in a previous report.[47] We speculate that a sufficient number of layers rather than lateral lamellar sizes are responsible for higher order reflections.

The small grain sizes in the sample can be explained by the asymmetric shape of the dyad molecule and thus unbalanced cross-sectional areas between the cubic POSS and discotic P5T molecules in the structure (see Figure 7a; the distance between lateral POSS molecules is larger than the parallel distance between the P5T molecules). In the POSS lamellar crystals, each POSS molecule had a cross-sectional area of 1.15 nm^2 (note that in the [001] projection of one hexagonal cell, there are two POSS molecules connecting to two P5T disks), whereas each P5T had a cross-sectional area of 0.63 nm^2 assuming its density was the same as in the bulk.[47] These unbalanced cross-sectional areas between covalently connected POSS and P5T would induce unbalanced stresses, as the POSS lamellar crystals would grow laterally. Because of a centrosymmetric arrangement of the P5T and POSS layers, no lamellae bending would be expected. A plausible option is that the POSS lamellar crystals have to break from time to time and the lateral grain sizes of the lamellar structure are thus small.

Figure 10B shows an example of the lamellar morphology for the 1:1 P5T−POSS:POSS blend. Obviously, the lamellar spacing is smaller than that for P5T−POSS in Figure 10A. This is consistent with the XRD results mentioned before. The grain size appears to be slightly larger (∼200 nm) than that for P5T−POSS, indicating a better crystal packing in the 1:1 P5T−POSS:POSS blend. This is possibly due to less unbalanced packing stresses in the POSS lamellar crystals, because the POSS molecules in the inner layers do not attach to any P5T molecules (see Figure 7b).

Computer Simulation of X-ray Diffraction. However, it is not certain whether ABCA four-layer POSS crystals will give the $(10\bar{1}1)$, $(11\bar{2}0)$, $(10\bar{1}2)$ and overlapped $(11\bar{2}3)/(30\bar{3}0)$ reflections. A computer calculation of the X-ray diffraction was carried out using MatLab 6.5. The model was built according to the unit cell dimensions obtained from XRD experiments and is demonstrated in Figure 11. The P5T discotic molecules were ignored in this model to avoid extra reflections. The sphere diameter was chosen as the POSS core diameter of ∼0.5 nm, and the molecules pack into an ABCA rhombohedral structure. The densities of the spheres, the interstitials between spheres, and the layer were arbitrarily chosen to be 1, 0, and −0.2, respectively, in the calculation. The computer-calculated X-ray profile completed after 3D fast Fourier transformation of the lattice and integration is shown in Figure 12. Reflections from both four-layer POSS crystals and the overall lamellar structure in the bottom simulation curve fitted well with those observed in the experimental XRD curve on the top. Because we did not include the disks in our model, the interdisk reflection was not seen in our calculated X-ray intensity profile. Also, only the $(10\bar{1}1)$, $(11\bar{2}0)$, $(10\bar{1}2)$, and overlapped $(11\bar{2}3)/(30\bar{3}0)$ reflections for POSS crystals were shown in the simulated

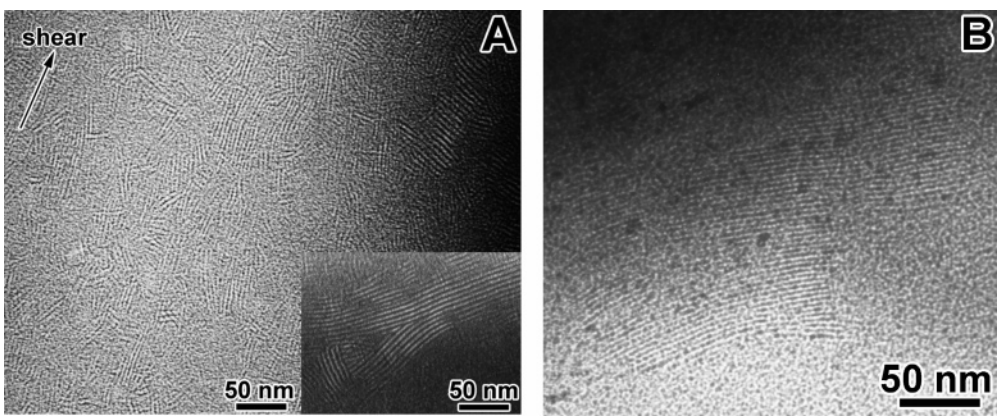

Figure 10. Bright-field TEM micrographs of (A) P5T−POSS and (B) 1:1 P5T−POSS:POSS. The inset in (A) has a higher magnification, showing the detailed structure of the lamellae. The thin sections were stained by RuO_4 for 30 min.

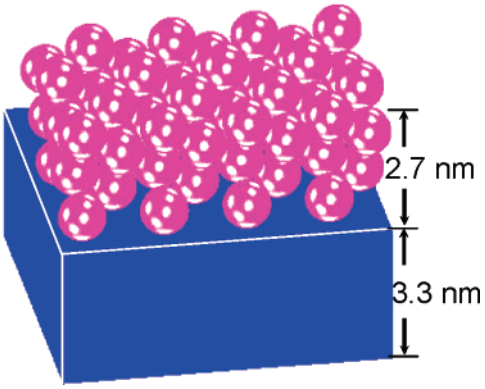

Figure 11. A computer simulation model on a 128 × 128 × 128 lattice for the self-assembled ABCA four-layer POSS lamellar crystal (2.7 nm) and a uniform amorphous layer of 3.3 nm thickness. The diameter of the spheres is 1.0 nm. The densities of the spheres and the amorphous lamella are arbitrarily chosen as 1 and −0.2, respectively. The empty space among the spheres has a density of zero.

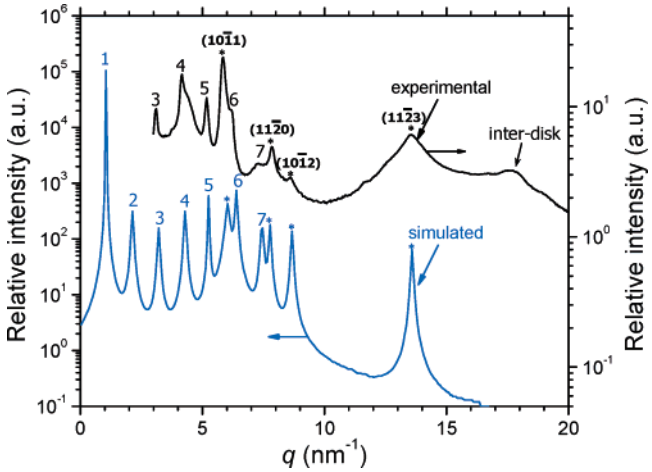

Figure 12. Computer-simulated X-ray intensity profile for the model in Figure 11, as compared with the experimental XRD data for P5T−POSS. The (11$\bar{2}$3) reflection is overlapped with the (30$\bar{3}$0) reflection.

XRD curve. Other reflections from POSS crystals and high lamellar reflections (>seventh order) were ignored to ease the comparison. From this simulation, it is interesting to see that only four layers of ABCA-stacked POSS crystals generate major X-ray reflections with sufficient intensity, reminiscent of layered silicate crystals.[48] The agreement of the simulation results with the experimental data further confirmed the proposed structures of P5T−POSS and 1:1 P5T−POSS:POSS in Figure 7.

Conclusions

In summary, an asymmetric P5T−POSS dyad molecule was successfully synthesized. On the basis of DSC, XRD, and TEM results, we observed nanophase separated liquid crystalline P5T and crystalline POSS lamellae in the neat P5T−POSS and a miscible 1:1 P5T−POSS:POSS blend. The P5T discotic molecules formed a bilayer lamella sandwiched between neighboring POSS lamellar crystals in P5T−POSS, whereas they interdigitated in the 1:1 P5T−POSS:POSS blend. Instead of forming columnar mesophases confined between the POSS layers, discotic P5T molecules assembled into a confined liquid crystalline phase with a parallel alignment of the disks to the layer normal (reminiscent of a homeotropic discotic nematic phase) in the neat P5T−POSS, whereas they were isotropic in the 1:1 P5T−POSS:POSS blend at room temperature (above the T_i at −5 °C). On the basis of 2D SAXS and WAXD results, we determined that the POSS molecules stacked into an ABCA four-layer lamella with the same rhombohedral crystal structure as that in 3D POSS crystals. Computer-simulated XRD results proved that a single layer of ABCA-stacked POSS molecules could produce major crystal reflections with *d*-spacings similar to those in the bulk POSS crystals. In the future, investigations on the effect of different spacer lengths and blending ratios will be carried out.

Acknowledgment. This work was supported by NSF CAREER award DMR-0348724, DuPont Young Professor Grant, and 3M Nontenured Faculty Award. L.Z. thanks Prof. Patrick T. Mather at Case Western Reserve University for stimulating discussion.

Supporting Information Available: DSC thermograms and 1D WAXD profiles of iB−POSS−OH and 11-undecanoyl iB−POSS. This material is available free of charge via the Internet at http://pubs.acs.org.

CM060394E

(46) Kim, J. K.; Lee, H. H.; Sakurai, S.; Aida, S.; Masamoto, J.; Nomura, S.; Kitagawa, Y.; Suda, Y. *Macromolecules* **1999**, *32*, 6707−6717.
(47) Cui, L.; Miao, J.; Zhu, L.; Sics, I.; Hsiao, B. S. *Macromolecules* **2005**, *38*, 3386−3394.
(48) *Crystal Structures of Clay Minerals and Their X-ray Identification*; Brindley, G. W., Brown, G., Eds.; Mineralogical Society: London, 1984.